Supporting Information
Kharenko et al.

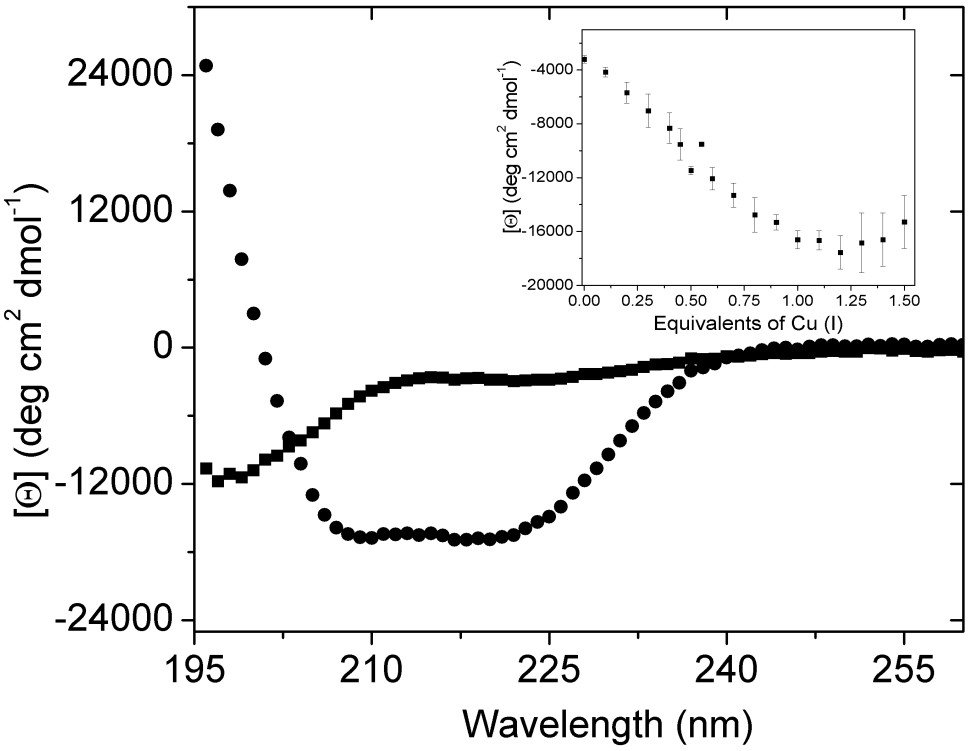

Figure S1. Far UV circular dichroism spectra of C16C19-GGY (236 μM) taken before (■) and after (●) the addition of Cu(I) (283 μM) in 0.2 M acetate buffer, pH 5.4 in the presence of 1 mM TCEP. Inset: Plot of θ_{222} as a function of added Cu(I).

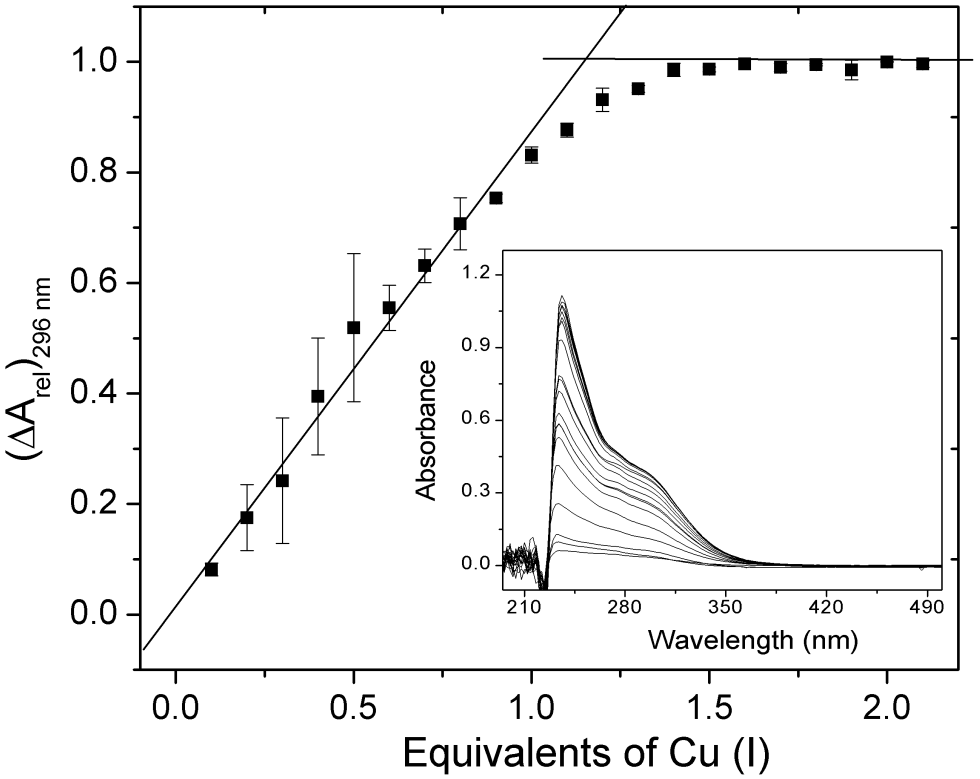

Figure S2. UV titration of 100 μM C16C19-GGY by Cu(I) in 0.2 M acetate buffer pH 5.4 500 μM TCEP. Inset: Difference spectra of the Cu(I)/C16C19-GGY solutions.

Supporting Information
Kharenko et al.

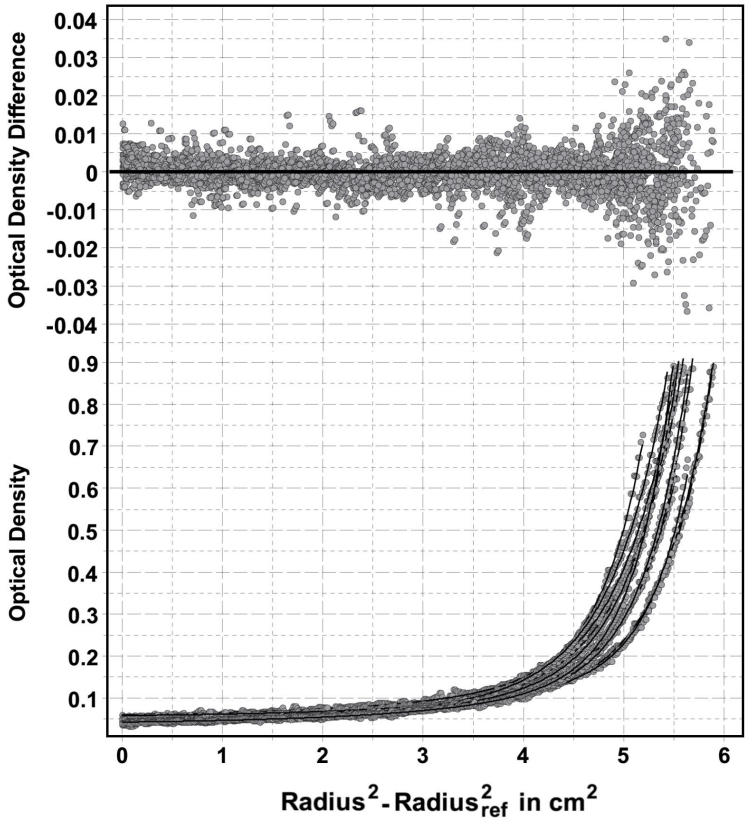

Figure S3. Residuals (top panel) and overlays (bottom panel) of a fit of the experimental equilibrium data from the Cu-C16C19GGY peptide to a "two-component ideal noninteracting" model. In the experiment, 280 nm scans were taken at equilibrium from 3 concentrations (200, 320 and 450 µM) and 4 different speeds (50.0, 53.3, 56.7 and 60.0 krpm) and globally analyzed with UltraScan (Demeler, B. (2005) UltraScan version 7.0) by fitting to self-associating and noninteracting models. The "two-component ideal noninteracting" model provided the best fit as judged by the variance and the residual run patterns, with the monomer-tetramer model being the next best candidate. The fit resulted in a species with a molecular weight of 2.9 kD, and a species with a molecular weight of 12.1 kD and a variance of 2.36 x 10^{-5}. The "monomer-tetramer" model resulted in a monomer molecular weight of 3.06 kD and a variance of 5.01 x 10^{-5}. The partial specific volume of C16C19GGY peptide was determined by the method of Cohn and Edsall (Cohn, E. J., and Edsall, J. T. (1943) Proteins, Amino Acids, and Peptides as Ions and Dipolar Ions. New York, Reinhold.) from the protein sequence of C16C19GGY peptide and found to be 0.7425 ccm/g.

Supporting Information
Kharenko et al.

XAS Data Collection and Analysis:

Copper K-edge XAS data for Cu-C16C19-GGY were collected on beam line X9B at the National Synchrotron Light Source at Brookhaven National Laboratory. The sample was placed in a polycarbonate sample holder and frozen in liquid nitrogen. For XAS data collection, the plastic sample holder was then inserted into an aluminum frame that was held near 50K by a He displex cryostat. Data were collected under ring conditions of 2.8 GeV and 120-300 mA using a sagitally focusing Si(111) double-crystal monochromator. Harmonic rejection was accomplished with a focusing mirror left flat. The X-ray energy of the focused monochromatic beam was internally calibrated to the first inflection of a Cu foil spectrum (8980.3 eV). X-ray fluorescence data were collected using a 13-element Ge detector (Canberra). X-ray absorption near-edge structure (XANES) data were collected from ca. 8780-9180 eV and X-ray absorption fine structure (EXAFS) were collected from 8780-10000 eV. For both sets of data the primary vertical aperture was set to 0.3mm.

The integrity of the samples was monitored by comparing XANES data from sequential scans. No significant changes were noted. Upon removal from the sample holder, visual inspection revealed that where the beam had been incident on the sample, the color had changed from colorless to yellow.

The XANES analysis was performed by fitting a baseline to the pre-edge and edge regions of the spectrum (*ca.* 8780 – 8960) using a cubic function for the pre-edge and 75% Gaussian and 25% Lorenzian function to fit the rise in fluorescence occurring at the edge. Gaussian functions were added for transitions occurring at lower energy and

the areas of the Gaussian fits were taken as peak areas. An average of *ca*. 3 scans (39 spectra with edge energy variation ≤ 0.2 eV) were used in the XANES analysis.

EXAFS data were analyzed using the program EXAFS123.[1] Eight scans were averaged to generate an EXAFS spectrum (edge energy variation ≤ 0.4 eV). The summed data files were background corrected and normalized using a five section cubic spline to fit the background in the pre-edge and post-edge regions. The data were converted to *k* space using the relationship $[2m_e(E-E_0)/\hbar^2]^{1/2}$ (where m_e is the electron mass, $\hbar$ is Plank's constant divided by 2π and E_0 is the threshold energy of the absorption edge, which was chosen to be 8990 eV. Least-squares fits of the EXAFS data over a *k* range of 2-12.5 $Å^{-1}$ were performed on Fourier-filtered data with a backtransform window = 1 – 4 Å. The upper limit of the *k* space range was limited by high-frequency noise. Best fits were generated by minimizing the goodness of fit criterion ($GOF = [n\{idp\}/(n\{idp\}-n\{p\})]^{1/2} R$, where *R* = avg [data simulation/esd(data)], *n(p)* is the number of varied parameters, and *n(idp)* is the number of data points for unfiltered refinements or $2(r_{max}-r_{min})(k_{max}-k_{min})\pi$ for filtered refinements).

Theoretical phases and amplitudes for EXAFS analyses were calculated using FEFF 8 and the crystallographically characterized model compounds: benzil bisthiosemicarbazonatocopper(II)[2], bis(μ_2-thiourea)-tetrakis(thiourea)-di-copper(I) bis(tetrafluoroborate)[3], and tetrakis(N-methylimidazole)copper(I) perchlorate[4].

Upon determining the first coordination sphere around the copper, additional scatterers were added to fit the FT between 2 and 4 Å. The number of copper atoms was initially allowed to refine, giving a value of 2.8 Cu atoms. This value was then locked to either two or three for subsequent fits. With the exception of the Cu scattering atoms, the

number of scattering atoms in a given fit were set to integer values and not allowed to refine. This led to three free-running parameters for each shell: the distance (r), the disorder parameter (σ^2) and E_0.

(1) Padden, K. M.; Krebs, J. F.; Trafford, K. T.; Yap, G. P. A.; Rheingold, A. H.; Borovik, A. S.; Scarrow, R. C. *Chem. Mater.* **2001**, *13*, 4305.
(2) Bushnell, G. W.; Tsang, A. Y. M. *Can. J. Chem.* **1979**, *57*, 603.
(3) Taylor, I. F.; Weininger, M. S.; Amma, E. L. *Inorg. Chem.* **1974**, *13*, 2835.
(4) Clegg, W.; Acott, S. R.; Garner, C. D. *Acta Crystallogr., Sect. C: Cryst. Struct. Commun.* **1984**, *40*, 768.

Supporting Information
Kharenko et al.

Table S1. Fits for Cu-C16C19-GGY Fourier-filtered Cu K-edge EXAFS Data (backtransform window of 1 - 4 Å.)

Shells	Radius (Å)	σ^2 (Å ^{2})	E(0)shift (eV)	GOF
1S	2.05(7)	0.007(4)	-15(15)	1.62
2S	2.10(6)	0.012(4)	-8(9)	1.47
3S	2.11(5)	0.016(4)	-8(8)	1.40
4S	2.10(5)	0.019(4)	-9(7)	1.38
5S	2.09(5)	0.021(4)	-10(7)	1.38
6S	2.08(5)	0.024(4)	-11(7)	1.39
1S	2.04(7)	0.006(4)	-16(16)	1.62
1Cu	2.81(4)	0.009(5)	79(0)	
2S	2.09(6)	0.012(4)	-8(9)	1.46
1Cu	2.81(6)	0.009(4)	77(8)	
3S	2.10(5)	0.016(4)	-8(8)	1.37
1Cu	2.80(5)	0.009(4)	77(7)	
4S	2.10(5)	0.019(4)	-9(7)	1.34
1Cu	2.80(5)	0.009(4)	76(7)	
1S	2.05(7)	0.007(4)	-14(16)	1.65
2Cu	2.87(9)	0.02(1)	82(7)	
2S	2.11(5)	0.012(4)	-6(8)	1.29
2Cu	2.87(5)	0.010(3)	12(9)	
3S	2.12(5)	0.016(3)	-5(6)	1.18
2Cu	2.86(5)	0.010(2)	12(8)	
4S	2.12(4)	0.019(3)	-6(5)	1.13
2Cu	2.86(5)	0.010(2)	12(8)	
1S	2.06(6)	0.007(4)	-12(14)	1.52
3Cu	2.87(6)	0.013(3)	13(8)	
2S	2.12(5)	0.013(4)	-5(8)	1.30
3Cu	2.86(5)	0.013(3)	12(8)	
3S	2.13(5)	0.016(3)	-5(6)	1.18
3Cu	2.86(5)	0.013(3)	11(7)	
1N	1.92(3)	-0.001(2)	15(8)	1.10

2S	2.18(4)	0.009(4)	-5(7)	
1Cu	2.88(4)	0.005(2)	14(9)	
1N	1.92(2)	-0.001(2)	18(6)	1.08
3S	2.16(4)	0.012(3)	-7(5)	
1Cu	2.87(4)	0.005(2)	13(9)	
1N	1.92(4)	0.000(3)	9(15)	1.15
1S	2.22(7)	0.005(5)	2(16)	
2Cu	2.87(4)	0.009(2)	13(7)	
1N	1.90(3)	0.000(2)	4(10)	1.08
2S	2.22(5)	0.013(4)	3(6)	
2Cu	2.87(4)	0.010(2)	12(7)	
1N	1.88(4)	0.001(2)	-2(11)	1.06
3S	2.22(5)	0.020(4)	4(5)	
2Cu	2.86(4)	0.009(2)	12(7)	
1N	1.92(4)	0.000(3)	9(15)	1.18
1S	2.22(7)	0.006(5)	3(15)	
3Cu	2.87(4)	0.013(3)	12(7)	
1N	1.90(3)	0.001(2)	5(10)	1.08
2S	2.22(5)	0.013(2)	4(6)	
3Cu	2.86(4)	0.013(4)	11(6)	
1N	1.88(4)	0.001(2)	-2(11)	1.06
3S	2.22(5)	0.019(4)	11(6)	
3Cu	2.86(4)	0.013(2)	4(4)	
1N	1.89(2)	0.001(1)	2(6)	0.62
2S	2.22(3)	0.013(2)	4(4)	
2Cu	2.86(1)	0.009(1)	11(4)	
1Cu	3.87(3)	0.001(1)	35(6)	
1N	1.89(1)	0.0004(7)	2(4)	0.37
2S	2.22(2)	0.013(2)	4(2)	
2Cu	2.88(1)	0.0085(7)	17(3)	
1Cu	3.91(1)	0.0009(7)	41(0)	
2S	3.54(3)	0.006(2)	-5(4)	
1N	1.90(3)	0.001(2)	3(10)	1.00
2S	2.22(4)	0.013(4)	4(6)	
2Cu	2.90(4)	0.009(2)	19(6)	
2S	3.55(4)	0.003(2)	-2(6)	